Electronic Supplementary Material (ESI) for CrystEngComm.

Supplementary information

Thermodynamic pathway between the non-polar and ferroelectric polymorphs of guanidinium ethoxysulfonate

Marcin Jarek[a] and Marek Szafrański[*b]

[a]*NanoBioMedical Centre, Adam Mickiewicz University in Poznań, Wszechnicy Piastowskiej 3, 61-614 Poznań, Poland*

[b]*Faculty of Physics, Adam Mickiewicz University in Poznań, Uniwersytetu Poznańskiego 2, 61-614 Poznań, Poland*

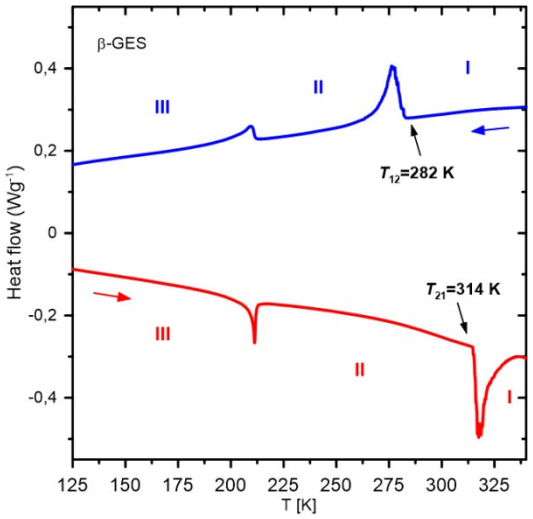

Fig. S1. DSC heating/cooling runs measured across the phase transitions region of β-GES. The temperature

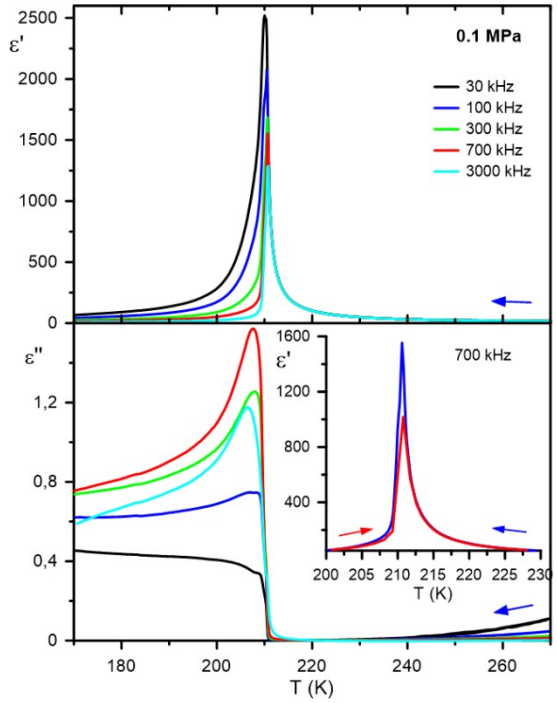

Fig. S2. Temperature and frequency dependences of the real (ε′) and imaginary (ε″) parts of the complex electric permittivity measured at ambient pressure. The inset shows the electric permittivity in the cooling and heating runs at 700 kHz frequency of the electric measuring field.

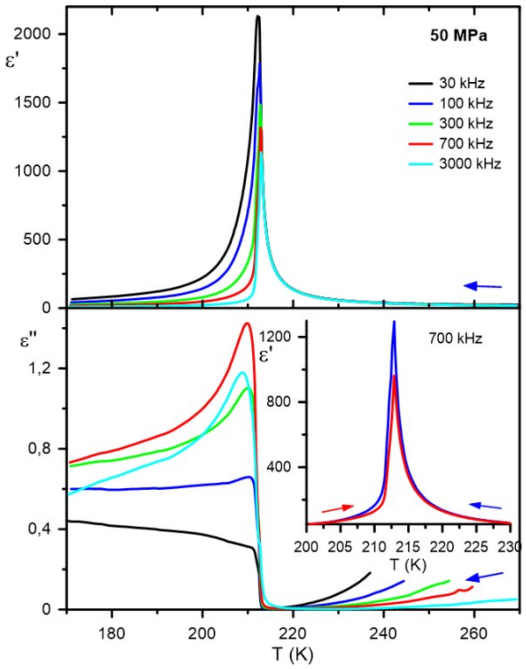

Fig. S3. Temperature and frequency dependences of the real (ε′) and imaginary (ε″) parts of the complex electric permittivity measured under pressure 50 MPa. The inset shows the electric permittivity in the cooling and heating runs at 700 kHz frequency of the electric measuring field.

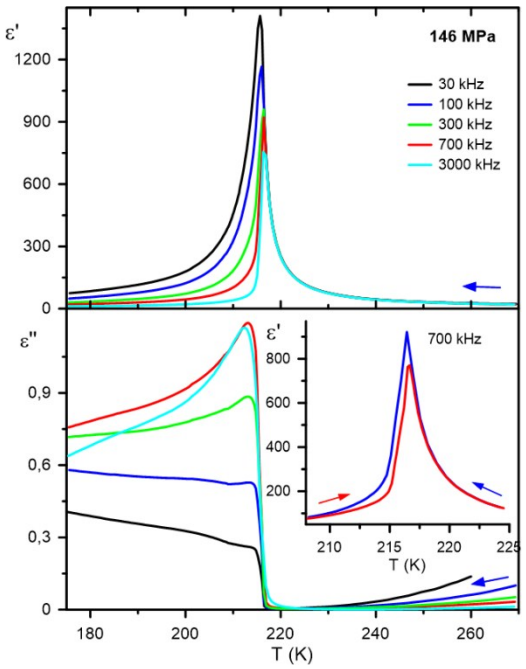

Fig. S4. Temperature and frequency dependences of the real (ε′) and imaginary (ε″) parts of the complex electric permittivity measured under pressure 146 MPa. The inset shows the electric permittivity in the cooling and heating runs at 700 kHz frequency of the electric measuring field.

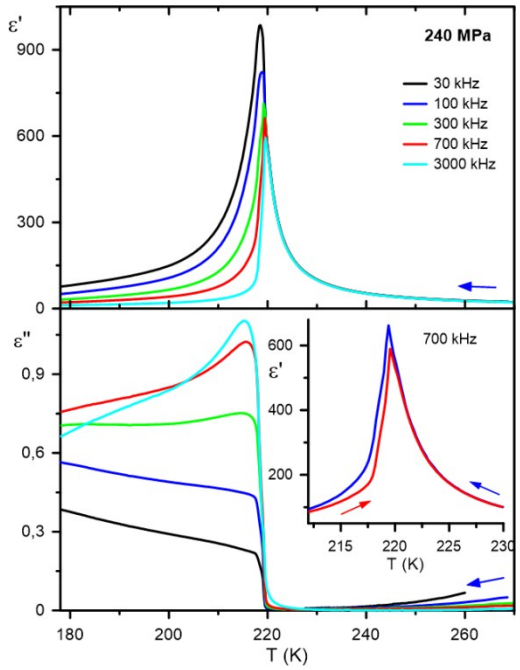

Fig. S5. Temperature and frequency dependences of the real (ε′) and imaginary (ε″) parts of the complex electric permittivity measured under pressure 240 MPa. The inset shows the electric permittivity in the cooling and heating runs at 700 kHz frequency of the electric measuring field.

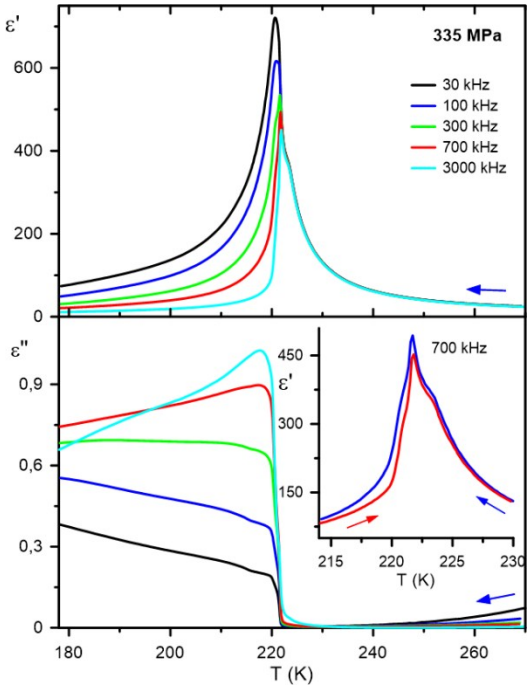

Fig. S6. Temperature and frequency dependences of the real (ε′) and imaginary (ε″) parts of the complex electric permittivity measured under pressure 335 MPa. The inset shows the electric permittivity in the cooling and heating runs at 700 kHz frequency of the electric measuring field.

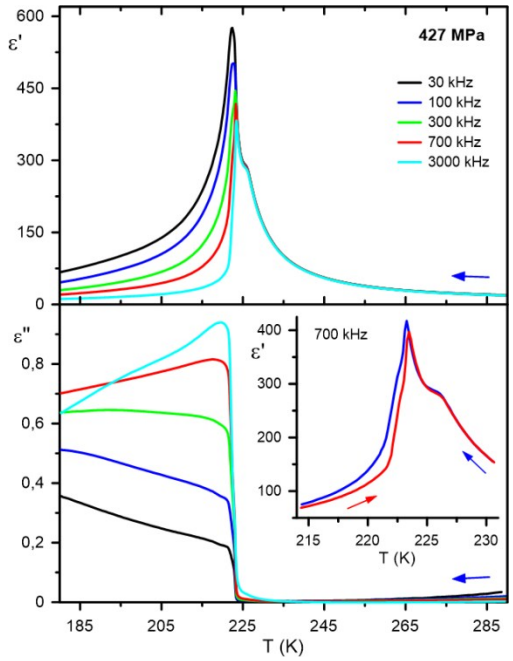

Fig. S7. Temperature and frequency dependences of the real (ε′) and imaginary (ε″) parts of the complex electric permittivity measured under pressure 427 MPa. The inset shows the electric permittivity in the cooling and heating runs at 700 kHz frequency of the electric measuring field.

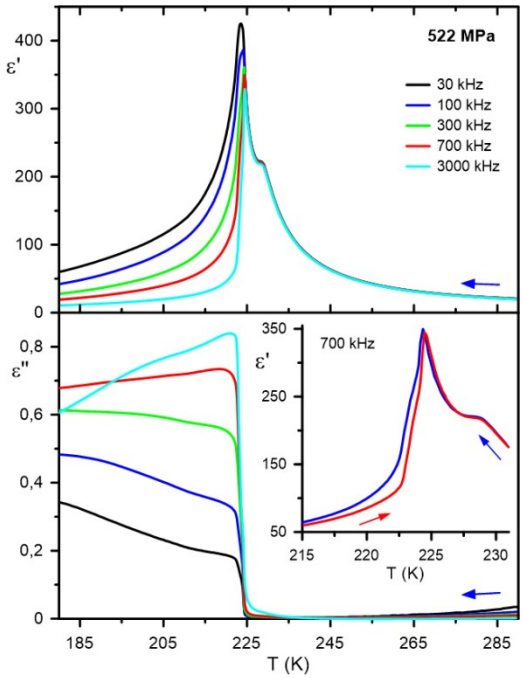

Fig. S8. Temperature and frequency dependences of the real (ε′) and imaginary (ε″) parts of the complex electric permittivity measured under pressure 522 MPa. The inset shows the electric permittivity in the cooling and heating runs at 700 kHz frequency of the electric measuring field.

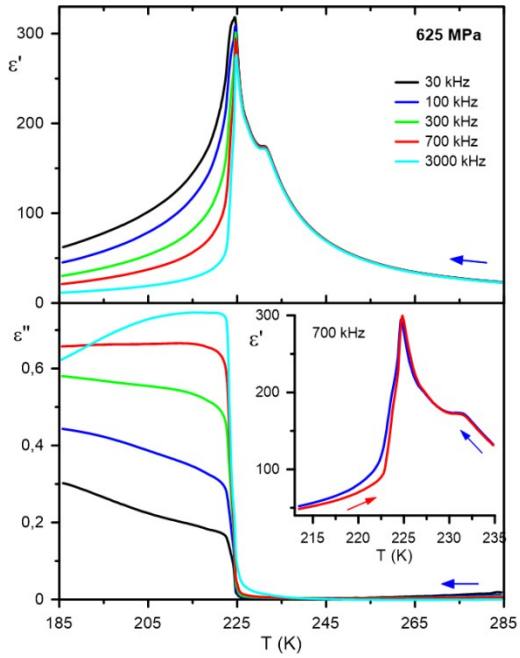

Fig. S9. Temperature and frequency dependences of the real (ε') and imaginary (ε") parts of the complex electric permittivity measured under pressure 625 MPa. The inset shows the electric permittivity in the cooling and heating runs at 700 kHz frequency of the electric measuring field.

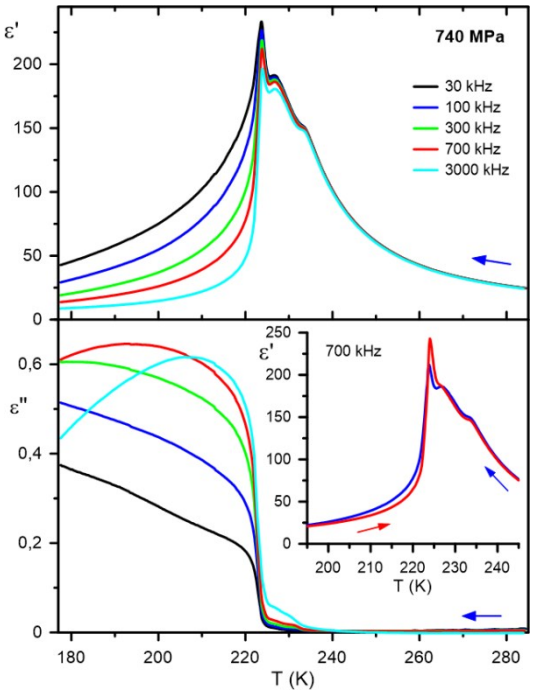

Fig. S10. Temperature and frequency dependences of the real (ε') and imaginary (ε") parts of the complex electric permittivity measured under pressure 740 MPa. The inset shows the electric permittivity in the cooling and heating runs at 700 kHz frequency of the electric measuring field.

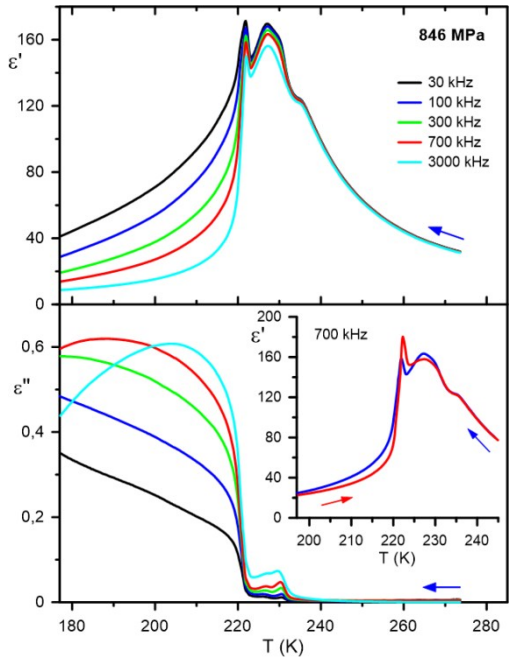

Fig. S11. Temperature and frequency dependences of the real (ε') and imaginary (ε") parts of the complex electric permittivity measured under pressure 846 MPa. The inset shows the electric permittivity in the cooling and heating runs at 700 kHz frequency of the electric measuring field.

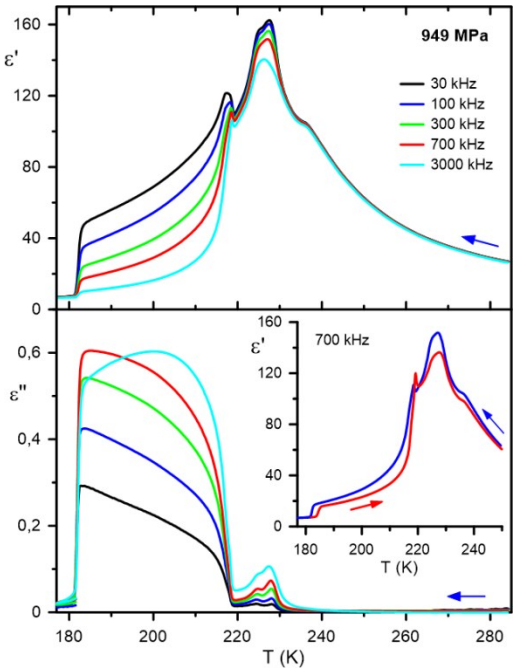

Fig. S12. Temperature and frequency dependences of the real (ε') and imaginary (ε") parts of the complex electric permittivity measured under pressure 949 MPa. The inset shows the electric permittivity in the cooling and heating runs at 700 kHz frequency of the electric measuring field.

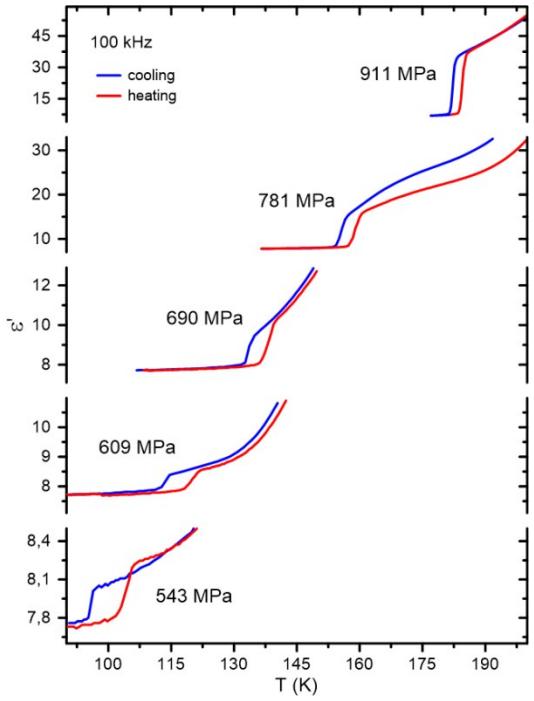

Fig. S13. Pressure dependence of the dielectric anomaly accompanying the transition between phases III and IV of β-GES.

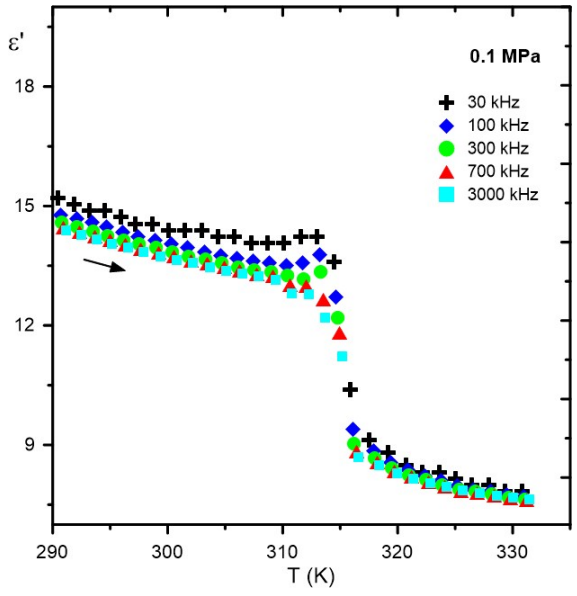

Fig. 14. Dielectric anomaly at the transition between phases II and I of β-GES.